Acta Cryst. (1983). A**39**, 1–13

Debye–Waller Factors of Zinc-Blende-Structure Materials – A Lattice Dynamical Comparison

BY JOHN S. REID

Department of Natural Philosophy, The University, Aberdeen AB9 2UE, Scotland

(*Received* 31 *March* 1982; *accepted* 26 *July* 1982)

Abstract

Lattice dynamical calculations to the full accuracy of the models are presented for the Debye–Waller B values for 17 zinc-blende-structure materials over the temperature range 1 to 1000 K (where appropriate). The materials are GaP, GaSb, GaAs, InP, InSb, InAs, ZnO, ZnS, ZnSe, ZnTe, CdTe, HgSe, HgTe, CuCl, CuBr, CuI and SiC. The models considered were the best lattice dynamical models available that have been fitted to phonon frequencies measured by neutron scattering. These include the shell model, the valence-shell model, the deformation-dipole model, the deformation-ion model and the rigid-ion model. From one to five models were used for each material, depending on the availability of published parameters. For some materials different parametrizations of the same model were examined. Intermodel comparisons show that the substantial difference in B values predicted by different models is attributable principally to the different eigenvectors they produce. Comparisons with fairly recent experimental results highlight the paucity of reliable measured values as a function of temperature and the unreliability and frequent inadequacy of models. The 14-parameter shell model is generally found to be the best.

Introduction

This account of the Debye–Waller factors has grown for several reasons to include 17 zinc-blende-structure materials. Since the earlier studies of Vetelino, Gaur & Mitra (1972) and Talwar & Agrawal (1974) there have become available a number of more sophisticated lattice dynamical models that fit measured phonon frequencies to good accuracy. The requirement of trustworthy Debye–Waller factors in calculations of TDS, LEED, EXAFS, impurity scattering, band structure and other fields suggested that the Debye–Waller factors given by these better models should be made available. The slowly increasing number of experimental investigations into the Debye–Waller factors of the zinc-blende-structure materials also requires a background of the best harmonic values against which the measured values can be assessed for consistency, anharmonicity and, possibly, dynamic deformation effects. Finally, the wide range of materials having this structure makes it particularly appropriate to use this group of materials to study the value of the Debye–Waller factor as a useful test of the reasonableness of the lattice dynamical models themselves. In particular, the Debye–Waller factors are sensitive to some aspects of the model eigenvectors. These are not directly measured or fitted by the inelastic neutron scattering experiments that are used to determine the models. Hence a good measurement of the Debye–Waller factors tests simply a feature of the models otherwise difficult to investigate. For this reason, all the good lattice dynamical models current in the literature have been included. It is hoped that one by-product of this study will be to provide further encouragement to those in a position to make reliable measurements of Debye–Waller B values as a function of temperature.

All the results given here, with the exception of the deformable-ion model predictions and those for the mercury compounds were presented at the XIIth International Congress of Crystallography (Reid, 1981).

The calculations

From the model frequencies $\omega(\mathbf{q}j)$ for wavevectors $\mathbf{q}$, and the eigenvectors $\mathscr{E}(k/\mathbf{q}j)$ for the k atom ($k = 1, 2$ for cation and anion), the Debye–Waller B_k can be expressed as usual as

$$B_k = \frac{8\pi^2}{3m_k} \cdot \frac{1}{N} \sum_{\mathbf{q}j} \left(\frac{E}{\omega^2} \right)_{\mathbf{q}j} |\mathscr{E}(k/\mathbf{q}j)|^2. \qquad (1)$$

$E_{\mathbf{q}j}$ is the energy in the mode $\mathbf{q}j$, m_k the mass of the kth atom and N the number of wavevectors in the summation over the Brillouin zone.

In the interests of simplicity, schemes for analytic manipulation of this expression to reduce the amount of irreducible eigendata required were avoided and the sum was evaluated directly. The expression already

0567-7394/83/010001-13$01.50

incorporates the cubic symmetry of the unit cell and allows diagonalization of the dynamical matrix to be restricted to 1/48th of the Brillouin zone, provided the multiplicity of symmetry-related **q** values in the rest of the zone is correctly accounted. The B values to be presented were all calculated with 12020 diagonalizations, equivalent to 3072000 terms contributing to the sum (1). Though such a large number is not necessary for reasonable accuracy, it ensures convergence to four decimal places, removing any doubt that the calculations themselves introduce error or that the zero-phonon contribution is inadequate.

Fig. 1 shows the typical convergence with increasing wavevector sample size. This sampling considerably exceeds the density employed by authors who have determined the mean-square vibrational amplitudes in a few of the source papers of the models to be quoted. Their results are generally worth recalculating, both to improve the accuracy and to introduce consistency in the intermodel comparisons.

Contrary to the estimates of Vetelino *et al.* (1972), it was found that the zero-phonon contribution is significant. The contribution of $\mathbf{q} = 0$ to (1) represents the average contribution over a volume $(1/N)$th of the whole zone surrounding $\mathbf{q} = 0$. If this 'zero-phonon' volume, V_Z, is divided into a very small number of subvolumes, as it would be with a very much larger choice of sampling density, and this division carried to indefinite limits, then the contribution (Z) of the zero-phonon volume becomes

$$Z = \frac{1}{V_Z} \cdot \frac{8\pi^2}{3Nm_k} \sum_j \int_{V_Z} \left(\frac{E}{\omega^2}\right)_{\mathbf{q}j} |\mathscr{E}(k/\mathbf{q}j)|^2 \, \mathrm{d}V_Z \quad (2)$$

$$= Z_A + Z_O, \quad (3)$$

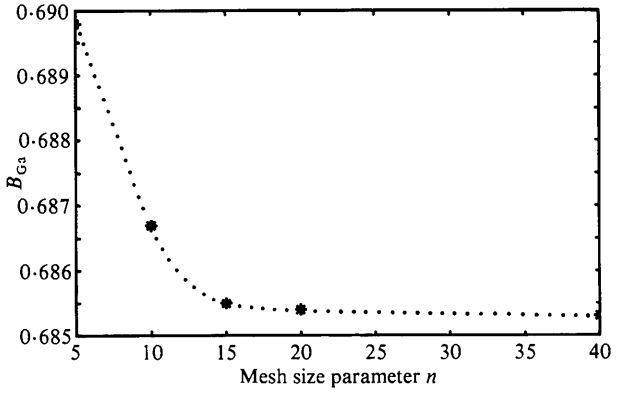

Fig. 1. A typical convergence of B with increasing wavevector sample size, shown here for B_{Ga} in GaAs. n is the number of sample wavevectors along [100] to the zone boundary on a uniform mesh covering the Brillouin zone. The total number of wavevectors in the sample is $N = (2n)^3$. The good convergence testifies to the effectiveness of the zero-phonon treatment since over 5% of the total B value is contributed by this one term with $n = 5$.

where Z_A represents the partial sum over acoustic modes and Z_O the partial sum over optic modes.

A slightly improved strategy was adopted for the evaluation of Z compared with the earlier work of Reid & Pirie (1980) on the group IV elements. A selection of over 200 small wavevectors in the dispersionless region was used to sample values of the integrand over a star of directions for all six branches. The optic average Z_O is simply evaluated, although it is very small compared with the acoustic term. The acoustic contribution from each branch depends on the average inverse square slope of the branches and the Debye integral term

$$\mathscr{F}(T) = \frac{kT}{\hbar\omega_{\max}} \int_0^{\hbar\omega_{\max}/kT} \frac{x\,\mathrm{d}x}{(e^x - 1)}, \quad (4)$$

Table 1. *A summary of the models investigated for each material*

The models are the 14-parameter shell model (SM); the 12-parameter valence-shell model (VSM); the deformable-ion model (DIM); the 15-parameter deformable-dipole model (DDM) and the 11-parameter rigid-ion model (RIM).

GaP	GaSb	GaAs	InP	InSb	InAs
SM[a]	SM(A)[d]	SM[f]	VSM[g]	SM[i]	VSM(A)[g]
VSM[b]	SM(B)[d]	VSM[b]	RIM[h]	VSM[g]	VSM(B)[g]
DDM[c]	VSM[b]	DDM[c]		DIM[j]	RIM[k]
RIM[c]	RIM[e]	RIM[c]		DDM[c]	
				RIM[c]	
ZnO	ZnS	ZnSe	ZnTe	CdTe	HgSe
VSM[b]	VSM(Ia)[l]	VSM[b]	VSM(I)[l]	SM(I)[o]	RIM[p]
	VSM(IIa)[l]	DDM[c]	VSM(II)[l]	SM(II)[o]	
	DIM[m]	RIM[c]	RIM[n]	RIM[n]	
	DDM[c]				
	RIM[c]				
HgTe	CuCl	CuBr	CuI	SiC	
DDM[q]	SM[r]	SM(I)[u]	SM[v]	DDM[c]	
RIM[q]	DDM[c]	SM(II)[u]	DDM[w]	RIM[c]	
	DIM[s]	RIM[t]	RIM[c]		
	RIM(1)[t]				
	RIM(2)[c]				

References: (*a*) Yarnell, Warren, Wenzel & Dean (1968), correction $\gamma_R = 0{\cdot}35452$ listed by Kunc & Nielsen (1979*b*); (*b*) Kunc & Biltz (1976); (*c*) Kunc, Balkanski & Nusimovici (1975*a*); (*d*) Farr, Taylor & Sinha (1975). Correction to model A: $\lambda = -0{\cdot}471$ (S. K. Sinha, private communication); (*e*) Vandevyver & Plumelle (1978); (*f*) Dolling & Waugh (1965); (*g*) Borcherds & Kunc (1978); (*h*) Vandevyver & Plumelle (1976); (*i*) Price, Rowe & Nicklow (1971); (*j*) Jaswal (1978*c*); (*k*) Talwar, Vandevyver & Zigone (1980); (*l*) Vagelatos, Wehe & King (1974); (*m*) Jaswal (1978*a*); (*n*) Plumelle and Vandevyver (1976); (*o*) Rowe, Nicklow, Price & Zanio (1974); (*p*) Kepa, Giebułtowicz, Burras, Lebech & Clausen (1982), parameters in private communication from H. Kepa; (*q*) Kepa *et al.* (1982), parameters from Kepa (1980); (*r*) Prevot, Hennion & Dorner (1977), published parameters are inadequate; those to full accuracy obtained from B. Prevot (private communication); (*s*) Jaswal (1978*b*); (*t*) Plumelle, Talwar, Vandevyver, Kunc & Zigone (1979). Correction for CuCl: $F_1 = -0{\cdot}022$ (M. Vandevyver, private communication); (*u*) Hoshino, Fujii, Harada & Axe (1976); (*v*) Prevot (1976); (*w*) reference (*c*) with correction $\gamma_1 = 0{\cdot}2332$ (K. Kunc, private communication).

which is evaluated numerically. The integral in (2) is, as usual, evaluated over a sphere of radius q_Z whose volume equals V_Z. Hence the zero-phonon term Z is entirely calculated from model data. Z decreases very slowly with increasing sample size, as $N^{-1/3}$, being about 1% of B at room temperature for $N = 0{\cdot}5 \times 10^6$. An accurate estimate of Z improves the convergence of B for increasing sampling density N.

Useful lattice dynamical information can be found by calculating the mass-averaged B value

$$\bar{B} = (m_1 B_1 + m_2 B_2)/(m_1 + m_2) \quad (5)$$

$$= \frac{8\pi^2}{3}\frac{1}{N}\sum_{qj}\left(\frac{E}{\omega^2}\right)_{qj}, \quad (6)$$

for it can be seen that the mass-averaged value $\bar{B}$ is independent of the eigenvectors.

When comparing model predictions it is convenient to select one model as reference and plot the percentage deviation of the other models from the reference model as a function of temperature for both B_1 (cation) and $\bar{B}$; *i.e.* to plot

$$\left.\begin{aligned} \Delta_1 &= (B_1^{\text{model}} - B_1^{\text{ref.}}) \times 100/B_1^{\text{ref.}} \\ \text{and} \\ \bar{\Delta} &= (\bar{B}^{\text{model}} - \bar{B}^{\text{ref.}}) \times 100/\bar{B}^{\text{ref.}} \end{aligned}\right\} \quad (7)$$

From measurements of these graphs (at the published scale) it is possible to recover to model B values to good accuracy using the inverse relationships:

$$B_1^{\text{model}} = B_1^{\text{ref.}}(1 + \Delta_1/100)$$

$$B_2^{\text{model}} = B_2^{\text{ref.}}(1 + \bar{\Delta}/100) + B_1^{\text{ref.}}\frac{m_1}{m_2}\frac{(\bar{\Delta} - \Delta_1)}{100}. \quad (8)$$

Although this presentation is inconvenient for those who wish tables of numbers, it both saves space and makes the intermodel comparisons much clearer.

Table 1 summarizes all the materials and the source lattice dynamical models considered here. These models are the best ones available, all having been fitted to phonon frequencies measured by neutron scattering. They were implemented using the subroutines of Kunc & Nielson (1979*a*,*b*) and Nielsen & Jaswal (1982). For five models, necessary corrections to the published parameters are given in the footnotes. Appendix *A* gives a very brief summary of the models for those who are interested in the results but are less familiar with the lattice dynamical background.

Results

Presentation

For most of the materials a shell model is taken as reference and its B values listed to four decimal places

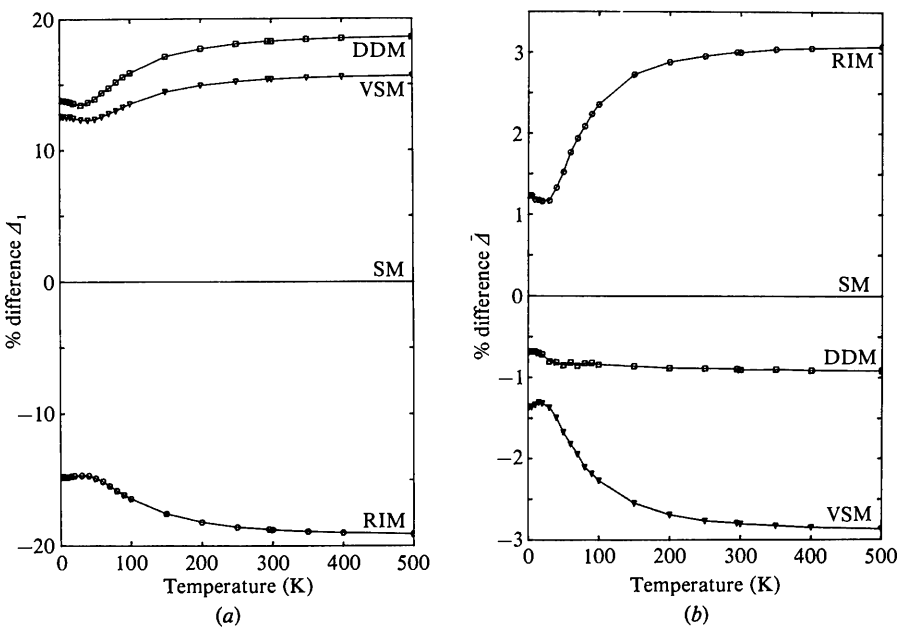

Temperature (K)	B_{Ga}	B_P
1·0	0·1291	0·1970
5·0	0·1292	0·1971
10·0	0·1296	0·1974
15·0	0·1302	0·1981
20·0	0·1312	0·1991
30·0	0·1349	0·2031
40·0	0·1409	0·2099
50·0	0·1491	0·2190
60·0	0·1588	0·2299
70·0	0·1699	0·2421
80·0	0·1819	0·2554
90·0	0·1946	0·2695
100·0	0·2080	0·2843
150·0	0·2802	0·3657
200·0	0·3576	0·4546
250·0	0·4373	0·5478
295·0	0·5101	0·6339
300·0	0·5183	0·6435
350·0	0·6000	0·7407
400·0	0·6823	0·8390
500·0	0·8478	1·0375
600·0	1·0140	1·2376
700·0	1·1806	1·4386
800·0	1·3475	1·6402
900·0	1·5146	1·8422
1000·0	1·6818	2·0445

Fig. 2. *General:* (*a*) Percentage difference of the Debye–Waller B for the cation (Ga in Fig. 2) between various models and the reference model. SM shell model (△); VSM valence-shell model (▽); DIM deformation-ion model (◇); DDM deformation-dipole model (□); RIM rigid-ion model (○). Experimental points, where plotted, are shown by an asterisk (*). (*b*) Percentage difference of the mass-averaged $\bar{B}$ value from equation (7) between various models and the reference model. *Particular:* GaP. Experimentally determined values for $\langle u^2 \rangle$ from 100 to 800 K are given by Bublik & Gorelik (1977) but no details of their experimental method are given nor an account of the corrections for any systematic errors. Only the shell model results here show a similar ratio of B values to their measured ratio. Table shows reference B values for shell model.

in the model table. This accuracy exceeds the significance of the model, especially considering the variance in the input parameters, but is useful for interpolation, extrapolation and comparison. The choice of shell model as reference is fairly arbitrary and does not imply that the shell model necessarily agrees best with any experimental data. The differences defined by (7) are shown in figures (*a*) and (*b*) for each material. More

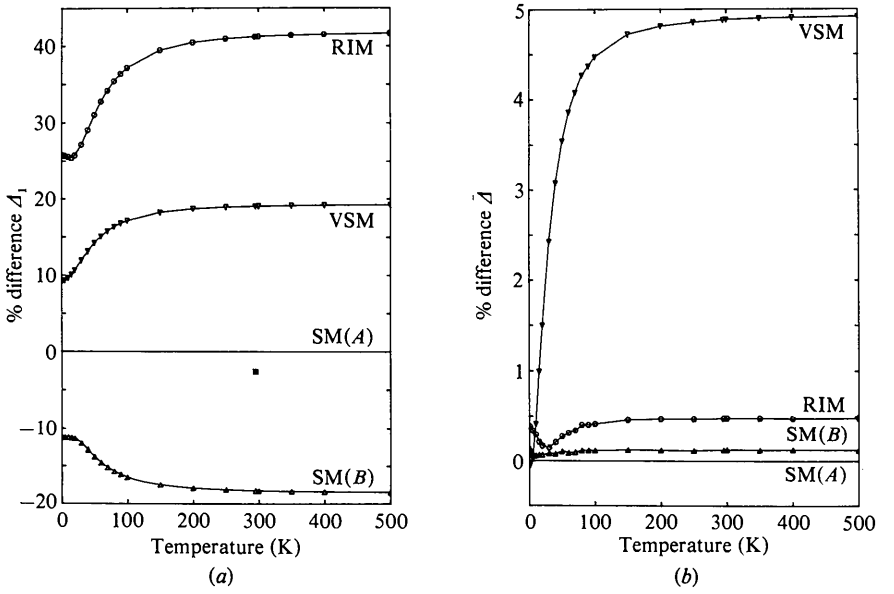

Temperature (K)	B_{Ga}	B_{Sb}
1·0	0·1614	0·1200
5·0	0·1617	0·1203
10·0	0·1627	0·1213
15·0	0·1651	0·1235
20·0	0·1694	0·1275
30·0	0·1831	0·1400
40·0	0·2016	0·1567
50·0	0·2228	0·1760
60·0	0·2460	0·1970
70·0	0·2706	0·2192
80·0	0·2961	0·2422
90·0	0·3225	0·2659
100·0	0·3496	0·2900
150·0	0·4911	0·4149
200·0	0·6382	0·5434
250·0	0·7878	0·6735
295·0	0·9237	0·7912
300·0	0·9388	0·8043
350·0	1·0906	0·9357
400·0	1·2429	1·0673
500·0	1·5485	1·3311
600·0	1·8548	1·5954
700·0	2·1615	1·8599
800·0	2·4685	2·1245
900·0	2·7757	2·3893

Fig. 3. *General:* as for Fig. 2. *Particular:* GaSb. The experimental point shown for B_{Ga} is from Morlon, Fukamachi & Hosoya (1981*a*,*b*). Their value for B_{Sb} is extremely low. The results of Bublik & Gorelik (1977) at room temperature are in quite good agreement with SM(*A*), both in respect of magnitude and ratio. SM(*B*) could not be distinguished from SM(*A*) by the originating authors on grounds of goodness of fit or interpretation of parameter values. It does, however, produce $B_{Ga} < B_{Sb}$, contrary to experimental results. Table shows reference B values for shell model (*A*).

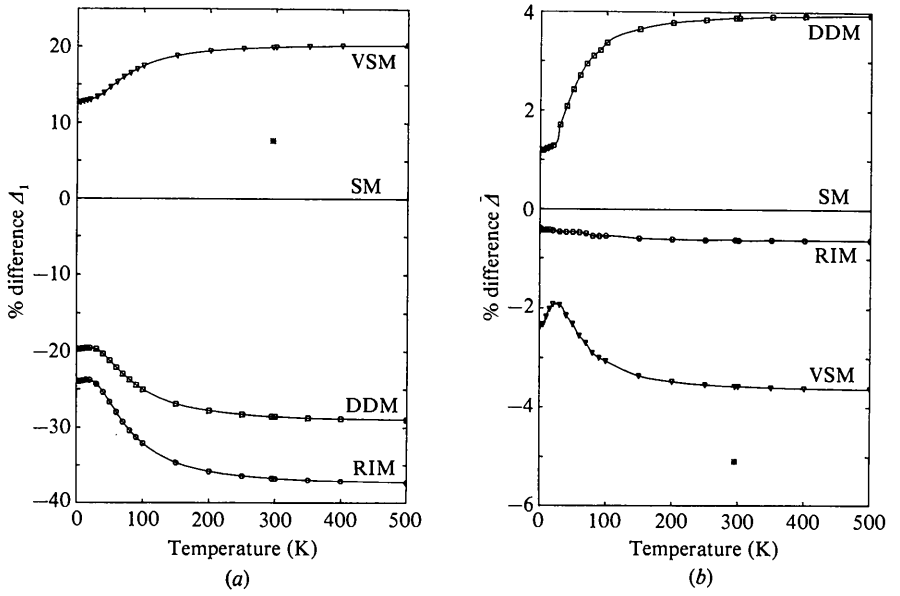

Temperature (K)	B_{Ga}	B_{As}
1·0	0·1385	0·1398
5·0	0·1387	0·1399
10·0	0·1392	0·1404
15·0	0·1402	0·1415
20·0	0·1422	0·1436
30·0	0·1489	0·1512
40·0	0·1590	0·1626
50·0	0·1714	0·1766
60·0	0·1855	0·1924
70·0	0·2008	0·2095
80·0	0·2171	0·2276
90·0	0·2341	0·2464
100·0	0·2516	0·2657
150·0	0·3452	0·3682
200·0	0·4439	0·4757
250·0	0·5451	0·5855
295·0	0·6373	0·6853
300·0	0·6476	0·6965
350·0	0·7509	0·8082
400·0	0·8547	0·9205
500·0	1·0632	1·1458
600·0	1·2725	1·3718
700·0	1·4822	1·5983
800·0	1·6921	1·8249
900·0	1·9023	2·0518
1000·0	2·1126	2·2787

Fig. 4. *General:* as for Fig. 2. *Particular:* GaAs. The experimental values are from G. J. McIntyre (to be published – private communication). Matsushita & Hagashi (1977) quote two possibilities for $\bar{B}$, the larger choice agreeing closely with McIntyre's value. Bublik & Gorelik (1977) confirm the ratio of B_{Ga}/B_{As} obtained by McIntyre, though their B results are lower. Only the VSM predicts $B_{Ga} > B_{As}$, as required by experiment, but its absolute values are not in particularly good agreement with experiment. Table shows reference B values for shell model C(ii).

recent experimental B values are also included on the graphs. Comments specific to one material are located in the figure caption for that material.

The figures are numbered as follows: Fig. 2 GaP; Fig. 3 GaSb; Fig. 4 GaAs; Fig. 5 InP; Fig. 6 InSb; Fig. 7 InAs; Fig. 8 ZnO; Fig. 9 ZnS; Fig. 10 ZnSe; Fig. 11 ZnTe; Fig. 12 CdTe; Fig. 13 HgSe; Fig. 14 HgTe; Fig. 15 CuCl; Fig. 16 CuBr; Fig. 17 CuI; Fig. 18 SiC.

With increasing temperature, the high-temperature limit is reached by a few hundred degrees K. The difference graphs then become horizontal for they contain no more information than a constant dif-

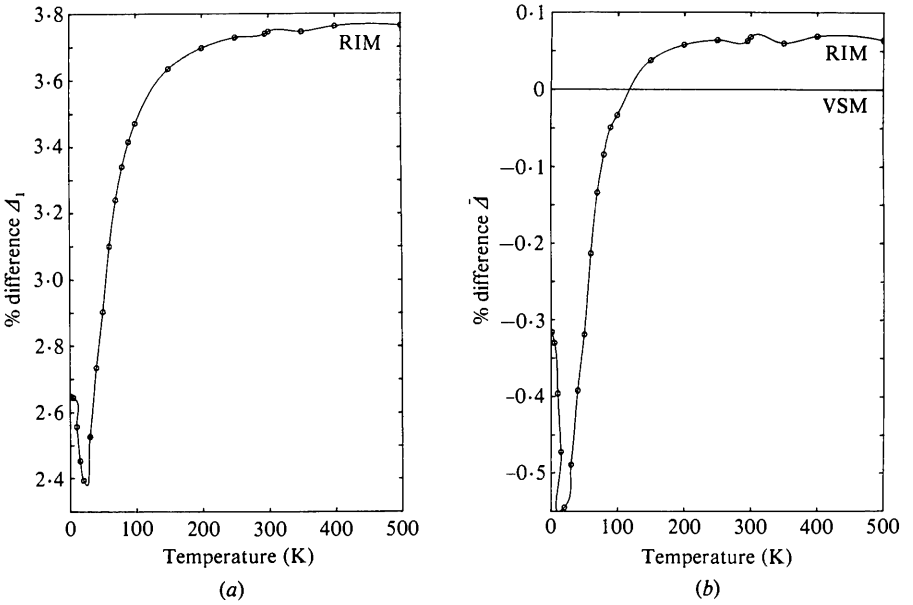

Temperature (K)	B_{In}	B_P
1·0	0·1397	0·1729
5·0	0·1399	0·1732
10·0	0·1408	0·1740
15·0	0·1427	0·1755
20·0	0·1462	0·1779
30·0	0·1582	0·1848
40·0	0·1755	0·1938
50·0	0·1963	0·2040
60·0	0·2193	0·2151
70·0	0·2438	0·2268
80·0	0·2694	0·2391
90·0	0·2957	0·2519
100·0	0·3226	0·2652
150·0	0·4622	0·3376
200·0	0·6057	0·4171
250·0	0·7509	0·5008
295·0	0·8824	0·5783
300·0	0·8970	0·5870
350·0	1·0437	0·6748
400·0	1·1906	0·7636
500·0	1·4851	0·9432
600·0	1·7800	1·1244
700·0	2·0752	1·3065
800·0	2·3705	1·4892
900·0	2·6660	1·6723
1000·0	2·9615	1·8556

Fig. 5. *General:* as for Fig. 2. *Particular:* InP. Both models make $B_{In} > B_P$ by a substantial amount, contrary to the results of Bublik & Gorelik (1977). The small kinks in the curves are insignificant artefacts of rounding to four decimal places. Table shows reference B values for valence-shell model.

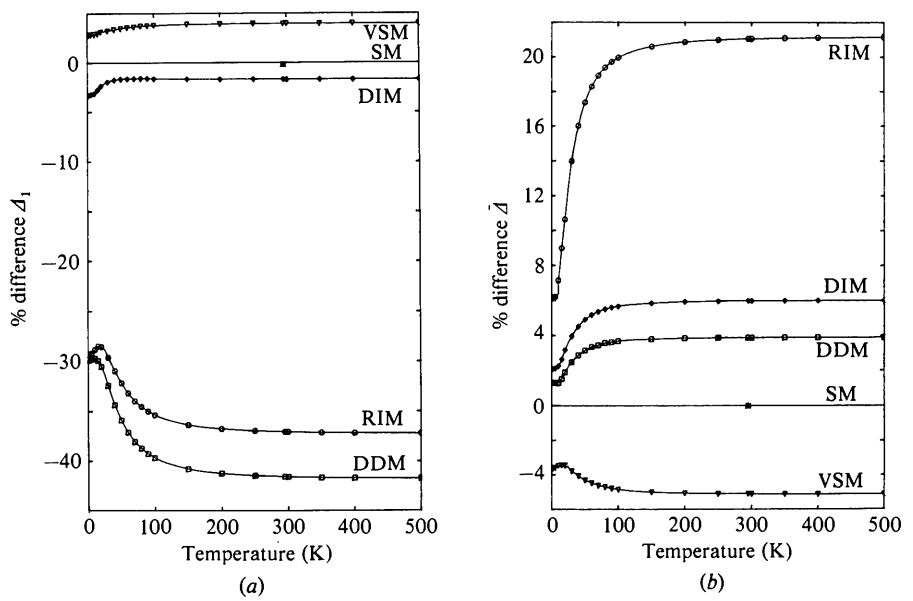

Temperature (K)	B_{In}	B_{Sb}
1·0	0·1561	0·1350
5·0	0·1566	0·1355
10·0	0·1591	0·1377
15·0	0·1654	0·1432
20·0	0·1755	0·1517
30·0	0·2036	0·1751
40·0	0·2376	0·2031
50·0	0·2748	0·2338
60·0	0·3141	0·2661
70·0	0·3547	0·2997
80·0	0·3962	0·3341
90·0	0·4385	0·3692
100·0	0·4814	0·4047
150·0	0·7004	0·5868
200·0	0·9233	0·7724
250·0	1·1479	0·9597
295·0	1·3508	1·1289
300·0	1·3734	1·1478
350·0	1·5994	1·3363
400·0	1·8257	1·5252
500·0	2·2789	1·9034
600·0	2·7325	2·2821
700·0	3·1864	2·6610
800·0	3·6405	3·0401

Fig. 6. *General:* as for Fig. 2. *Particular:* InSb. The experimental points are a conversion of Θ_M values given by Bilderback & Colella (1976). Both Kyutt (1975) and Bublick & Gorelik (1977) obtain approximately the same ratio for B_{In}/B_{Sb}, this ratio being similar to that given by the shell model only. However, Kyutt and Bublik & Gorelik do not agree about the magnitude or temperature dependence of the B values. Table shows reference B values for shell model.

ference between Debye temperatures. Should harmonic predictions for the B's be required at elevated temperatures up to the melting point or phase transition they can be obtained to full accuracy by linear extrapolation of the data presented. (See Appendix B for a comment on Debye temperatures for these materials.)

Comparisons with experiment

The comparison of experimental results and theoretical calculations of B values is so fraught with difficulty that no attempt has been made to mark error bars on the graphs that include recent experimental values. On the experimental side, it is clear from experience with better-studied materials that in addition to the random errors generally quoted there are unknown but possibly substantial systematic errors arising from the various assumptions made in processing the raw data to obtain the B values. Work done during the past decade has tried to correct deficiencies in previous approaches but, in the absence of a study of these systematic errors, merely considering the quoted statistical errors is misleading. In the most careful studies, authors tend to quote standard errors of between 0·5 and 1·5%.

On the theoretical side, the scene is equally disastrous for different reasons. One cannot estimate properly the variance of B even for models with quoted parameter errors, for the parameters are correlated by unquoted amounts. In the absence of pairwise covariances for the parameters, insufficient statistical detail is available to answer the relevant question: 'If a new set of frequencies were remeasured with comparable accuracy, a model refitted with similar parameters, by how much would one expect the new B values to differ from the ones calculated here?' The refitting process necessary to provide the answer was considered excessively lengthy. To obtain a qualitative guide, a set of random deviations were made to the parameters for GaSb based on the quoted errors. The resulting dispersion curves were examined to see if they remained reasonable. These deviations typically produced B values different by a few percent with

Temperature (K)	B_{Zn}	B_O
1·0	0·1426	0·2164
5·0	0·1428	0·2165
10·0	0·1431	0·2168
15·0	0·1437	0·2174
20·0	0·1446	0·2182
30·0	0·1478	0·2207
40·0	0·1533	0·2245
50·0	0·1610	0·2292
60·0	0·1706	0·2349
70·0	0·1816	0·2411
80·0	0·1937	0·2479
90·0	0·2068	0·2551
100·0	0·2205	0·2627
150·0	0·2958	0·3054
200·0	0·3769	0·3546
250·0	0·4607	0·4085
295·0	0·5374	0·4600
300·0	0·5459	0·4658
350·0	0·6320	0·5255
400·0	0·7186	0·5867
500·0	0·8927	0·7125
600·0	1·0677	0·8411
700·0	1·2431	0·9713
800·0	1·4188	1·1026
900·0	1·5947	1·2347
1000·0	1·7707	1·3672

Fig. 8. ZnO. B values for valence-shell model.

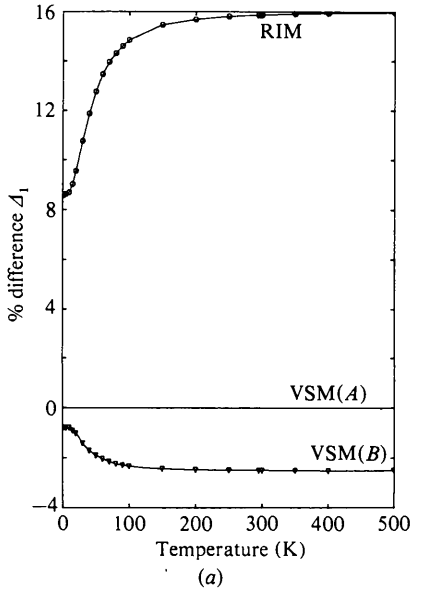

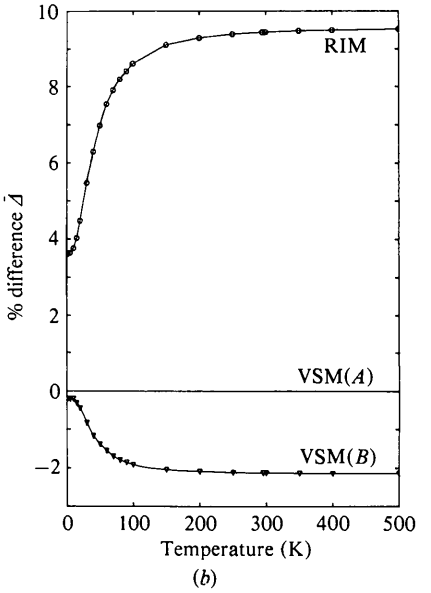

Temperature (K)	B_{In}	B_{As}
1·0	0·1387	0·1240
5·0	0·1390	0·1243
10·0	0·1402	0·1254
15·0	0·1429	0·1276
20·0	0·1476	0·1310
30·0	0·1626	0·1406
40·0	0·1828	0·1530
50·0	0·2062	0·1670
60·0	0·2316	0·1821
70·0	0·2585	0·1983
80·0	0·2864	0·2151
90·0	0·3150	0·2326
100·0	0·3441	0·2506
150·0	0·4945	0·3458
200·0	0·6489	0·4458
250·0	0·8049	0·5481
295·0	0·9461	0·6412
300·0	0·9618	0·6516
350·0	1·1192	0·7559
400·0	1·2770	0·8606
500·0	1·5930	1·0709
600·0	1·9095	1·2820
700·0	2·2263	1·4934
800·0	2·5432	1·7051
900·0	2·8603	1·9169
1000·0	3·1774	2·1288

Fig. 7. *General:* as for Fig. 2. *Particular:* InAs. The two valence-shell models given similar results. All models generate B_{In} appreciably greater than B_{As} compared with the slight excess in the results of Bubik & Gorelik (1977). Table shows reference B values for valence-shell model (A).

moderate, but not complete, correlation in the changes for the two ions.

Some further comparisons between independent model calculations and recent experiment, arising out of studies of ^{119}Sn impurity Debye–Waller-factor data in the III–V semiconductor elements only, are made by Nielsen, Larsen, Damgaard, Petersen & Weyer (1982).

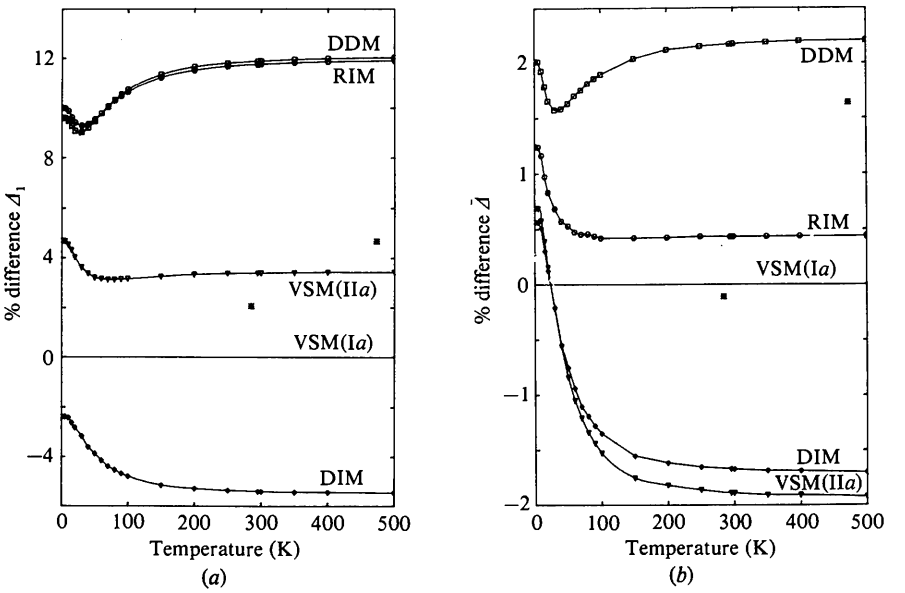

Temperature (K)	B_{Zn}	B_S
1·0	0·1728	0·2004
5·0	0·1730	0·2006
10·0	0·1739	0·2015
15·0	0·1756	0·2031
20·0	0·1783	0·2055
30·0	0·1872	0·2129
40·0	0·2007	0·2235
50·0	0·2176	0·2363
60·0	0·2370	0·2508
70·0	0·2582	0·2665
80·0	0·2807	0·2832
90·0	0·3042	0·3007
100·0	0·3285	0·3189
150·0	0·4570	0·4173
200·0	0·5915	0·5237
250·0	0·7288	0·6345
295·0	0·8537	0·7363
300·0	0·8676	0·7477
350·0	1·0072	0·8626
400·0	1·1473	0·9784
500·0	1·4287	1·2120
600·0	1·7108	1·4472
700·0	1·9933	1·6833
800·0	2·2762	1·9199
900·0	2·5592	2·1570
1000·0	2·8424	2·3943

Fig. 9. *General:* as for Fig. 2. *Particular:* ZnS. The experimental results are those of Moss, McMullan & Koetzle (1980) at 285 and 473 K and Cooper, Rouse & Fuess (1973) at 295 K. Vagelatos *et al.* (1974), who originated the valence-shell models for ZnS, favoured the 'high-Z' model VSM(II*a*) although it includes very large deformation charge values *d*. The comparison here suggests that VSM(I*a*), an equally good fit to the phonon data, is preferable, particularly in regard to B_S. The DIM, which produces very good dispersion curves by fitting only six parameters, gives B values rather close together for the two ions in the high-temperature limit. It has the interesting feature that B_S is 20% greater than B_{Zn} at low temperatures but 4% less than B_{Zn} at high temperatures. Table shows reference B values for valence-shell model (I*a*).

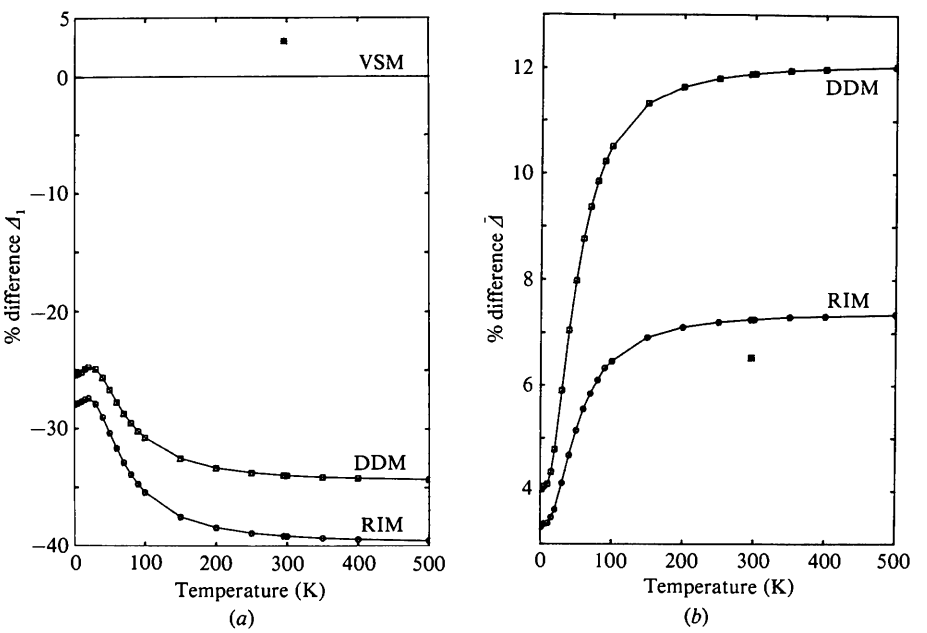

Temperature (K)	B_{Zn}	B_{Se}
1·0	0·1833	0·1312
5·0	0·1835	0·1314
10·0	0·1845	0·1323
15·0	0·1865	0·1340
20·0	0·1900	0·1368
30·0	0·2022	0·1453
40·0	0·2198	0·1570
50·0	0·2411	0·1709
60·0	0·2649	0·1863
70·0	0·2906	0·2029
80·0	0·3175	0·2204
90·0	0·3454	0·2386
100·0	0·3741	0·2574
150·0	0·5249	0·3568
200·0	0·6820	0·4610
250·0	0·8418	0·5675
295·0	0·9869	0·6644
300·0	1·0031	0·6752
350·0	1·1653	0·7835
400·0	1·3280	0·8924
500·0	1·6545	1·1109
600·0	1·9818	1·3301
700·0	2·3095	1·5496
800·0	2·6375	1·7694
900·0	2·9658	1·9894
1000·0	3·2941	2·2094

Fig. 10. *General:* as for Fig. 2. *Particular:* ZnSe. The experimental points are from the X-ray study of McIntyre, Moss & Barnea (1980). Only the valence shell model is in reasonable agreement with these values. Table shows reference B values for valence-shell model.

Interpretation

At all temperatures the B values represent a sum over eigendata weighted towards the lower frequencies, the weighting shifting with increasing temperature to emphasize the low-frequency contribution. This shift in weighting is responsible for the generally greater difference between models at high temperatures, reflecting a large variation in the low-frequency predictions of the models. From a lattice dynamical point of view this is at first surprising because different treatment by the models of atomic polarizability and short-range forces is primarily aimed at accounting for behaviour away from the dispersionless region. The origin of the effect lies with several factors: the relative paucity of data at low frequencies because measurements are made at

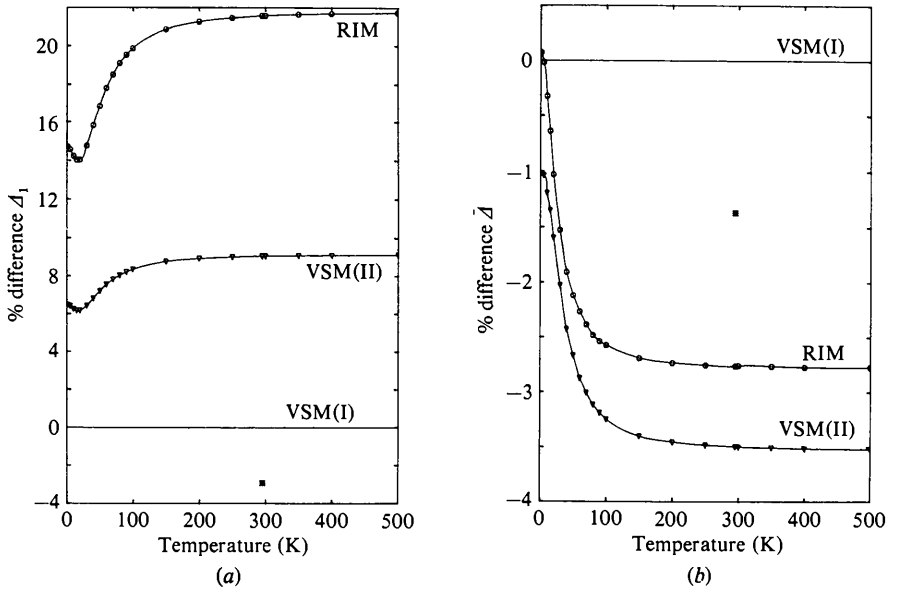

Temperature (K)	B_{Zn}	B_{Te}
1·0	0·2037	0·1252
5·0	0·2043	0·1257
10·0	0·2064	0·1277
15·0	0·2110	0·1317
20·0	0·2186	0·1380
30·0	0·2410	0·1556
40·0	0·2697	0·1778
50·0	0·3023	0·2025
60·0	0·3374	0·2290
70·0	0·3745	0·2567
80·0	0·4129	0·2853
90·0	0·4524	0·3145
100·0	0·4928	0·3441
150·0	0·7021	0·4967
200·0	0·9180	0·6527
250·0	1·1367	0·8103
295·0	1·3348	0·9528
300·0	1·3569	0·9686
350·0	1·5780	1·1274
400·0	1·7997	1·2865
500·0	2·2440	1·6052
600·0	2·6892	1·9243
700·0	3·1348	2·2437
800·0	3·5807	2·5632
900·0	4·0268	2·8828
1000·0	4·4730	3·2025

Fig. 11. *General:* as for Fig. 2. *Particular:* ZnTe. The experimental points from Cooper *et al.* (1973) marginally favour VSM(I), the 'low-Z' model of Vagelatos *et al.* (1974). As with ZnS, this choice is not that made by Vagelatos *et al.* though the results here suggest that the B values should be seriously considered when deciding on a 'best' model. Table shows reference B values for the valence-shell model (I).

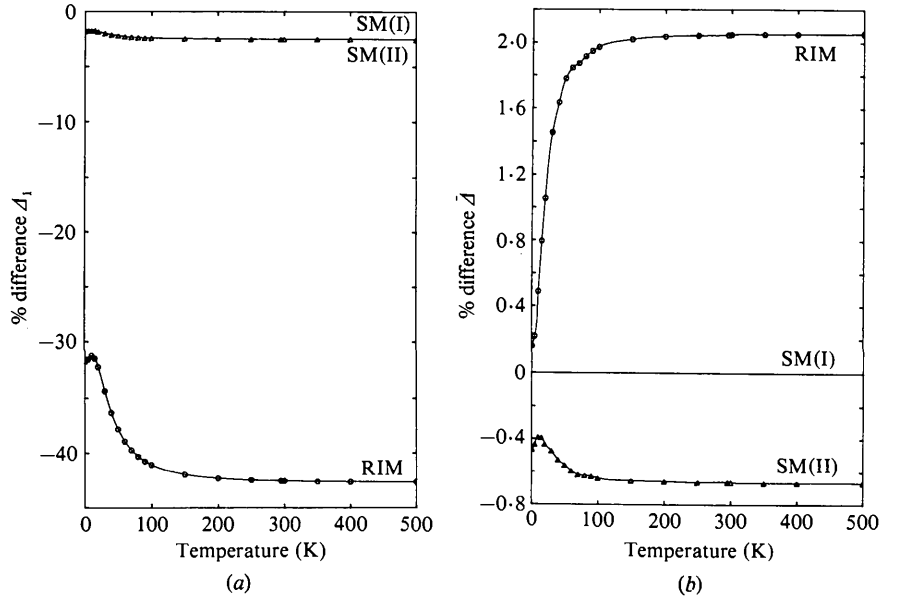

Temperature (K)	B_{Cd}	B_{Te}
1·0	0·1905	0·1388
5·0	0·1913	0·1396
10·0	0·1957	0·1431
15·0	0·2066	0·1508
20·0	0·2232	0·1620
30·0	0·2668	0·1905
40·0	0·3179	0·2237
50·0	0·3731	0·2595
60·0	0·4307	0·2971
70·0	0·4900	0·3360
80·0	0·5504	0·3757
90·0	0·6116	0·4160
100·0	0·6734	0·4569
150·0	0·9876	0·6656
200·0	1·3060	0·8778
250·0	1·6262	1·0916
295·0	1·9151	1·2847
300·0	1·9472	1·3062
350·0	2·2688	1·5213
400·0	2·5907	1·7366
500·0	3·2351	2·1678
600·0	3·8799	2·5994
700·0	4·5250	3·0313
800·0	5·1703	3·4633
900·0	5·8157	3·8954
1000·0	6·4611	4·3276

Fig. 12. *General:* as for Fig. 2. *Particular:* CdTe. SM(II) fitted the piezoelectric constant (e_{14}) whereas SM(I) did not. The results here confirm that the two models are lattice dynamically very similar. Table shows reference B values for the valence-shell model (I).

equispaced wavevectors; the higher susceptibility of the lower frequencies to the importance of systematic spectrometer instrumental resolution corrections and, finally, the variation in fitting procedure particularly with regard to the incorporation or absence of elastic constant data.

Looking broadly over the graphs (*a*) which reflect the variations in individual B values between models, one cannot but be surprised at the wide range of predictions for most materials. This is not a happy situation if one wishes to select a theoretical value for use, as is necessary for many of the materials in the absence of reliable experimental values. From the lattice dynamical viewpoint it is most encouraging for it highlights that the Debye–Waller factor provides a stringent test of the reasonableness of a model although it is only an average quantity. Looking over the graphs (*b*) for the mass-averaged $\bar{B}$ values one sees a level of agreement amongst models almost an order of magnitude better. Since $\bar{B}$ depends only on the eigenfrequencies, this confirms that the models are indeed consistently good fits to the experimental phonon frequencies and squarely attributes the differences between the individual B_k values to the eigenvector ratio $|\mathscr{E}(1/\mathbf{q}j)|^2/|\mathscr{E}(2/\mathbf{q}j)|^2$ representing the ratio of displacement amplitudes of the ions.

Some general remarks can be made about intermodel comparisons. The mass averaged $\bar{B}$ from the 14-parameter rigid-ion models (RIM) are within a few percent of the shell model values for more than half of the materials, though the individual B values differ by typically 30%. The 15-parameter deformation-dipole models (DDM) tend to show similar discrepancies to the rigid-ion models. One concludes that there are distinctive features of the dynamical matrix for each model which lead to restrictions on the character of the predicted eigenvectors regardless of reasonable parametrizations of the model. However, the RIM and DDM are equally likely to produce positive or negative differences with the shell model. The valence-shell model (VSM) predictions on the other hand are nearly

Temperature (K)	B_{Hg}	B_{Se}
1·0	0·2132	0·1570
5·0	0·2157	0·1585
10·0	0·2368	0·1665
15·0	0·2763	0·1801
20·0	0·3252	0·1965
30·0	0·4359	0·2332
40·0	0·5546	0·2727
50·0	0·6770	0·3139
60·0	0·8015	0·3567
70·0	0·9272	0·4008
80·0	1·0538	0·4458
90·0	1·1809	0·4916
100·0	1·3084	0·5381
150·0	1·9493	0·7766
200·0	2·5927	1·0204
250·0	3·2371	1·2665
295·0	3·8175	1·4891
300·0	3·8820	1·5138
350·0	4·5273	1·7619
400·0	5·1727	2·0105
500·0	6·4640	2·5084

Fig. 13. HgSe. B values for non-central rigid-ion model.

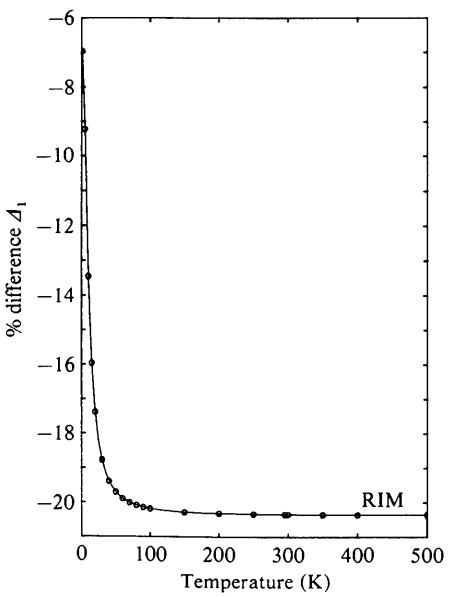

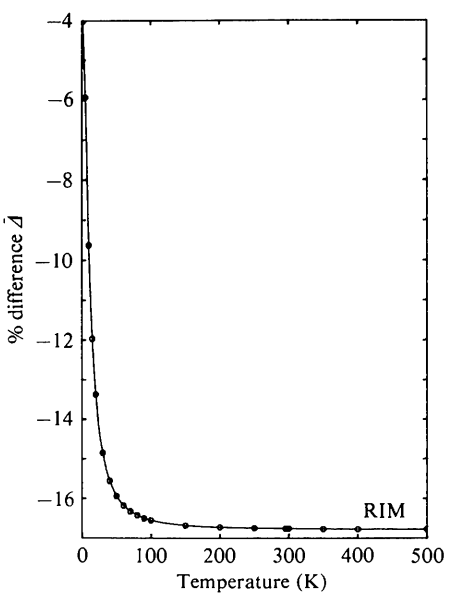

Temperature (K)	B_{Hg}	B_{Te}
1·0	0·2381	0·1313
5·0	0·2484	0·1343
10·0	0·2943	0·1468
15·0	0·3622	0·1656
20·0	0·4401	0·1873
30·0	0·6089	0·2346
40·0	0·7855	0·2847
50·0	0·9658	0·3368
60·0	1·1481	0·3903
70·0	1·3316	0·4448
80·0	1·5159	0·5002
90·0	1·7008	0·5563
100·0	1·8861	0·6127
150·0	2·8159	0·8994
200·0	3·7482	1·1897
250·0	4·6815	1·4814
295·0	5·5220	1·7447
300·0	5·6154	1·7740
350·0	6·5495	2·0670
400·0	7·4839	2·3603
500·0	9·3529	2·9474

Fig. 14. *General:* as for Fig. 2. *Particular:* HgTe. The models of Kepa *et al.* (1982) (see Table 1) for HgTe and HgSe are all very sensitive to lattice constant, particularly with respect to transverse acoustic branches. The DDM model for HgTe in particular shows a rapid decrease of many of these frequencies with decreasing lattice constant. This may be precursive of the transition of these materials to the cinnabar structure under pressure. Table shows reference B values for deformation-dipole model.

always larger than those of the 14-parameter shell models. The DIM models look sufficiently promising to merit a more systematic study.

Since the experimental results available tend to support the shell model predictions, it seems reasonable to suggest that the RIM and DDM have something

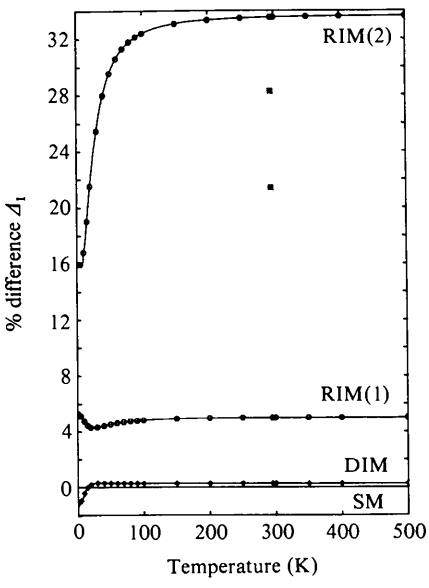

(*a*)

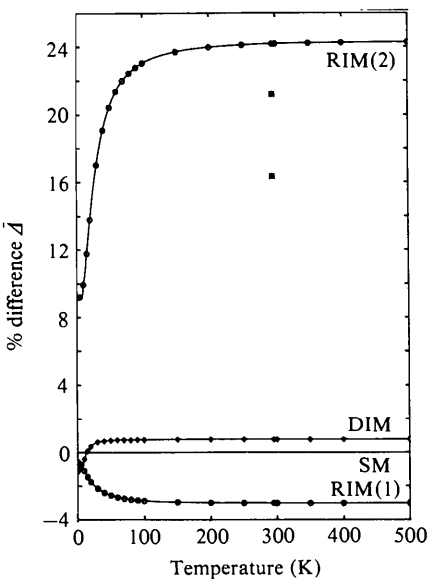

(*b*)

Temperature (K)	B_{Cu}	B_{Cl}
1·0	0·3638	0·3132
5·0	0·3653	0·3146
10·0	0·3723	0·3204
15·0	0·3907	0·3331
20·0	0·4203	0·3522
30·0	0·5009	0·4019
40·0	0·5973	0·4599
50·0	0·7019	0·5222
60·0	0·8113	0·5873
70·0	0·9239	0·6546
80·0	1·0386	0·7236
90·0	1·1548	0·7939
100·0	1·2721	0·8654
150·0	1·8679	1·2339
200·0	2·4712	1·6126
250·0	3·0776	1·9963
295·0	3·6248	2·3439
300·0	3·6856	2·3826
350·0	4·2946	2·7705
400·0	4·9041	3·1594
500·0	6·1243	3·9389
600·0	7·3453	4·7200
700·0	8·5667	5·5018

Fig. 15. *General:* as for Fig. 2. *Particular:* CuCl. Experimental points are from the neutron results of Sakata, Hoshino & Harada (1974), the lower values, and the X-ray results of Valvoda & Jecny (1978), the upper values. The observed B is substantially larger for copper than that given by most models, possibly indicating that the copper ions have a significant mobility or disorder displacement at room temperature. The SM, DIM and RIM(1) were fitted to 4·2 K phonon frequencies whereas RIM(2) was determined from a different room-temperature study. The DDM is not shown because with the parameters of Kunc *et al.* (1975*a*) it is unstable in some off-symmetry regions. (Kunc attributes this feature to the use of erroneous experimental input data.) Table shows reference B values for shell model.

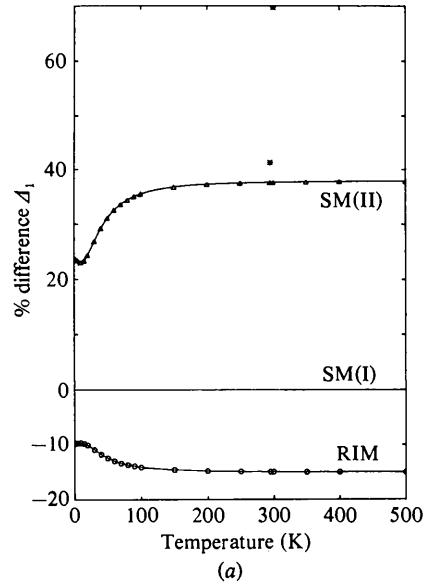

(*a*)

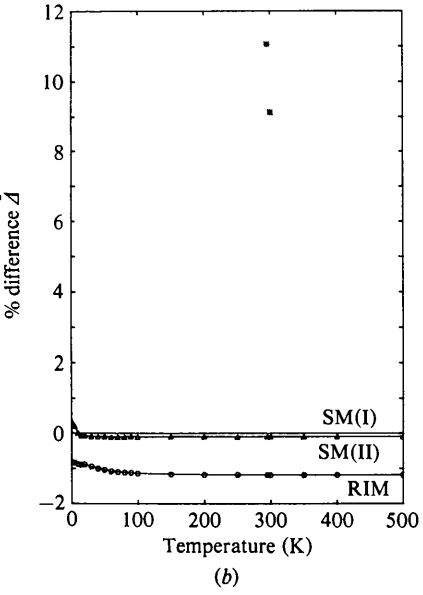

(*b*)

Temperature (K)	B_{Cu}	B_{Br}
1·0	0·2373	0·2828
5·0	0·2389	0·2844
10·0	0·2449	0·2915
15·0	0·2570	0·3077
20·0	0·2741	0·3324
30·0	0·3176	0·3977
40·0	0·3681	0·4746
50·0	0·4227	0·5576
60·0	0·4801	0·6445
70·0	0·5397	0·7337
80·0	0·6008	0·8247
90·0	0·6630	0·9168
100·0	0·7262	1·0099
150·0	1·0503	1·4825
200·0	1·3814	1·9612
250·0	1·7155	2·4423
295·0	2·0175	2·8765
300·0	2·0511	2·9248
350·0	2·3877	3·4080
400·0	2·7248	3·8917
500·0	3·4001	4·8598
600·0	4·0763	5·8287
700·0	4·7529	6·7979

Fig. 16. *General:* as for Fig. 2. *Particular:* CuBr. Experimental points from Harada, Suzuki & Hoshino (1976) at 300 K and Butt, Rouse & Thomas (1978) confirm that as with CuCl the B value for Cu is much greater than that given by the models. Indeed, the discrepancy is the largest of the three copper halides suggesting a mobility of the copper sublattice that makes the interpretation of a lattice dynamical model questionable. Table shows reference B values for shell model (I).

inherently unsuitable in their dynamical matrices, a feature that could not be detected from merely fitting to phonon frequencies. Since all the models actually have more parameters than those fitted, the remaining ones being chosen as zero or set equal to the others by assumption, it appears that the assumptions made in implementing these models need serious reconsideration. In the case of the DDM this conclusion lends strong support to Kunc's own suggestion (Kunc, Balkanski & Nusimovici, 1975*a*,*b*) that the deformable-bond approximation should be dropped in future work with this model.

It is also very clear for these materials, some of the simplest for which the eigenvectors play a significant role in the Debye–Waller factors, that no model generally produces acceptable agreement with those

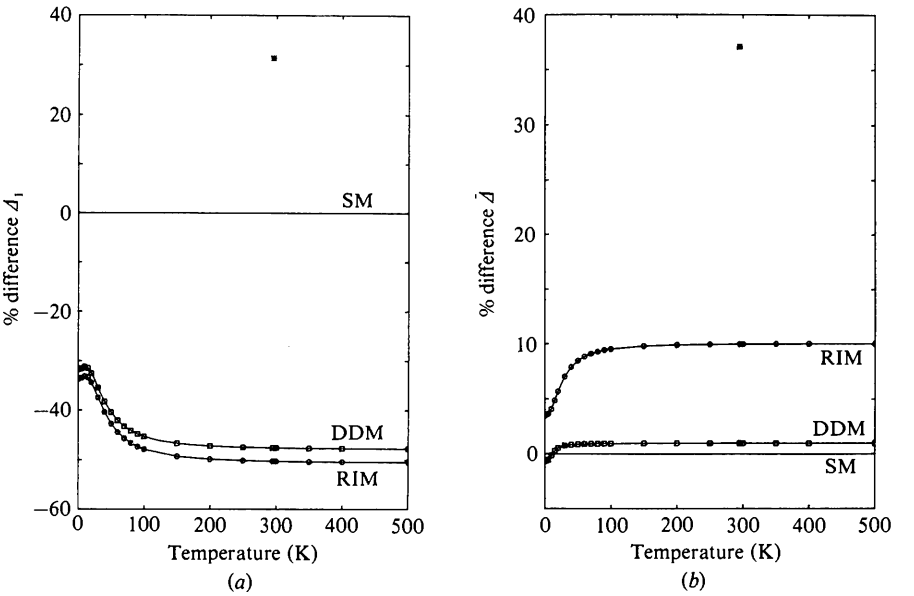

Temperature (K)	B_{Cu}	B_I
1·0	0·2886	0·1523
5·0	0·2895	0·1532
10·0	0·2938	0·1567
15·0	0·3051	0·1641
20·0	0·3234	0·1752
30·0	0·3742	0·2046
40·0	0·4357	0·2396
50·0	0·5032	0·2780
60·0	0·5746	0·3184
70·0	0·6486	0·3602
80·0	0·7245	0·4031
90·0	0·8017	0·4467
100·0	0·8800	0·4908
150·0	1·2803	0·7159
200·0	1·6879	0·9448
250·0	2·0987	1·1753
295·0	2·4697	1·3834
300·0	2·5110	1·4066
350·0	2·9242	1·6383
400·0	3·3381	1·8704
500·0	4·1668	2·3350
600·0	4·9964	2·8000
700·0	5·8264	3·2653

Fig. 17. *General:* as for Fig. 2. *Particular:* CuI. Experimental points from Morlon *et al.* (1981*a*). No great accuracy is claimed in this experiment using the anomalous scattering and no systematic corrections were made for diffuse scattering. Nonetheless the results continue to show an appreciable excess of B_{Cu} of experimental values over model predictions for the copper halides not at variance with their known superionic conductivities at higher temperatures. Table shows reference B values for shell model.

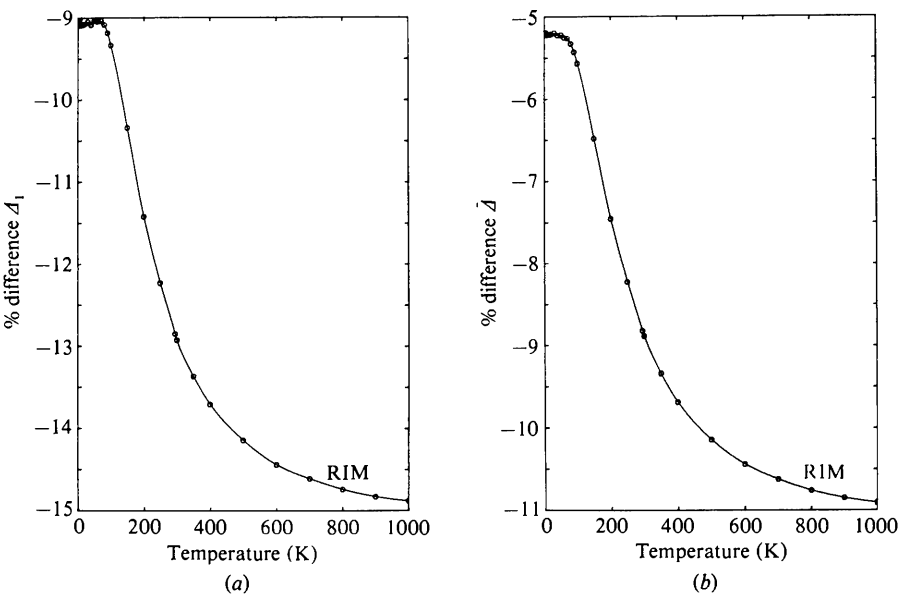

Temperature (K)	B_{Si}	B_C
1·0	0·1286	0·1677
5·0	0·1286	0·1677
10·0	0·1287	0·1677
15·0	0·1288	0·1678
20·0	0·1289	0·1679
30·0	0·1293	0·1683
40·0	0·1299	0·1688
50·0	0·1306	0·1695
60·0	0·1316	0·1704
70·0	0·1328	0·1714
80·0	0·1343	0·1726
90·0	0·1361	0·1740
100·0	0·1382	0·1755
150·0	0·1528	0·1850
200·0	0·1725	0·1971
250·0	0·1954	0·2115
295·0	0·2179	0·2261
300·0	0·2205	0·2278
350·0	0·2469	0·2458
400·0	0·2743	0·2650
500·0	0·3309	0·3064
600·0	0·3892	0·3505
700·0	0·4484	0·3964
800·0	0·5082	0·4435
900·0	0·5685	0·4915
1000·0	0·6290	0·5402

Fig. 18. *General:* as for Fig. 2. *Particular:* SiC. Table shows reference B values for deformation dipole model.

experimental results available. Though the current generation of models is much superior to the previous generation, they cannot be considered as the last word, particularly in their present parametrizations. Many models fit the dispersion curves well, as measured by a gross statistic like χ^2, but an examination of the residuals even by eye shows systematic trends both within and across materials. These differences are on the scale of a few percent. As far as the Debye–Waller factors are concerned the disagreement with available experimental results is generally by much larger amounts.

I am very grateful to Ole Holm Nielsen for allowing the use of his DIM subroutines prior to publication.

APPENDIX A
The models used

The shell model (SM) was originally based on the idea that each ion could be represented by a core which moved with the nucleus and a massless charged shell which represented (outer) electrons that moved significantly differently. Therefore, each atom was represented by two entities. Short-range harmonic forces were included between all entities involving first- and second-neighbour ions. Long-range electrostatic forces were included using Coulomb coefficients. The model was soon recast into the less pictorial language of a general second-order expansion of the lattice dynamical energy in terms of atomic displacements and induced dipoles. The apparently more general approach contained no terms missing in the first formulation though the convenient parameters were now somewhat different. In this form there are about 41 parameters that could be used for a zinc-blende-structure material. This large number was reduced to 14 by Dolling & Waugh (1965) when considering the material GaAs. The reduction was based on some (subjective) physical argument and a fair amount of arbitrary choice. Almost all subsequent work with the shell model for the zinc blende structure and the group IV elements has used Dolling & Waugh's 14-parameter version of the shell model.

The valence-shell model (VSM) considers that the important short-range degrees of freedom are associated with bond bending and stretching of linked groups of ions. Hence the large number of degrees of freedom in the shell model is reduced by trying to identify appropriate linear combinations of motions to parametrize. The 12 parameters of the standard valence-shell model can be used to generate an equivalent shell model which does not, however, satisfy the Dolling & Waugh criteria.

The deformation dipole model (DDM) was formulated independently of the shell model, notably by Hardy and Karo (*e.g.* Hardy, 1962), and differs principally in its method of treating the instantaneous total dipole moment in a unit cell. More recently the model has been generalized by Kunc et al. (1975*a*,*b*) and in this form should be similar to a general shell model. However, in its actual implementation for the zinc-blende-structure materials simplifications have been made, guided by plausible physical arguments, which reduce the number of parameters to 15 in the so-called 'deformable-bond approximation'. These simplifications include the neglect of 'non-local polarizabilities', giving a model that is different from the implementation of the shell model.

The deformation ion model (DIM) is the only model in which some of the long-range electrostatic forces are considered to be screened by a high-frquency dielectric constant. In addition, some further polarizability parameters are included over those present in the implementation of the DDM. The short-range forces have generally been treated as valence forces and a combination of physical insight and *ad hoc* assumptions used to reduce the numbers of adjustable parameters for a given material to a number less than ten.

The rigid-ion model (RIM) includes long-range electrostatic forces but no ionic polarizability. It cannot therefore give a satisfactory account of properties like the dielectric constant. Nevertheless the rigid-ion model is a surprisingly good fit to the dispersion curves of many zinc-blende-structure materials. The only arbitrary assumption is one of range of the forces and there is some degree of self balancing in that the ionic charge controls the ratio of long-range to short-range forces. There are no equivalent sets of force constants that produce identical frequencies and eigenvectors and for this and other reasons the model is the only workable one that can be used to investigate substitutional impurities. Not surprisingly, it is generally the first model to be applied to a material and is the only model for which, in simple versions, previous theoretical studies of the Debye–Waller factors for zinc-blende-structure materials have been made.

APPENDIX B
Debye temperatures

Debye temperatures have not been mentioned in the text although they are frequently mentioned in the literature concerning mean-square displacements of zinc-blende-structure materials. The Debye model is strictly for one atom per unit cell, where the B value does not depend on the displacement eigenvectors. In a standard notation (*e.g.* Willis & Pryor, 1975), the Debye temperature Θ_M is related to B by

$$B = \frac{6h^2}{mk_B}\frac{T}{\Theta_M^2}\left[\frac{T}{\Theta_M}\int_0^{\Theta_M/T}\frac{x\,\mathrm{d}x}{(e^x-1)} + \tfrac{1}{4}\frac{\Theta_M}{T}\right]. \qquad (B1)$$

At least three different ways of using this equation for zinc-blende-structure materials can be identified in the literature:

(*a*) Use of Θ_M as a single parameter to express the temperature variation of B_k. This is valid in the high-temperature limit. Setting $B_k \rightarrow B$ and $m_k \rightarrow m$ in ($B1$) gives a different Θ_M for each atom type.

(*b*) Using the result of (6) that $\bar{B}$ is independent of eigenvectors and of the same form as that in a monatomic cubic crystal. Setting $\bar{B} \rightarrow B$ and $(m_1 + m_2) \rightarrow m$ in ($B1$) gives Θ_M for $\bar{B}$.

(*c*) Using the linear temperature dependence of the Debye model to fit (an average) dB_k/dT and setting $(1/m_1 + 1/m_2)/2 \rightarrow 1/m$ in ($B1$).

Other schemes could be in use, for authors often fail to mention the details of their conversion to Debye temperatures. Care should be taken in interpretating published figures.

References

BILDERBACK, D. H. & COLELLA, R. (1976). *Phys. Rev. B*, **6**, 2479–2488.

BORCHERDS, P. H. & KUNC, K. (1978). *J. Phys. C*, **11**, 4145–4155.

BUBLIK, V. T. & GORELIK, S. S. (1977). *Krist. Tech.* **12**, 859–869.

BUTT, N. M., ROUSE, K. D. & THOMAS, M. W. (1978). *Acta Cryst.* A**34**, 759–761.

COOPER, M. J., ROUSE, K. D. & FUESS, H. (1973). *Acta Cryst.* A**29**, 49–56.

DOLLING, G. & WAUGH, J. L. T. (1965). *Lattice Dynamics*, edited by R. F. WALLIS, pp. 19–32. Oxford: Pergamon.

FARR, M. K., TRAYLOR, J. G. & SINHA, S. K. (1975). *Phys. Rev. B*, **11**, 1587–1594.

HARADA, J., SUZUKI, H. & HOSHINO, S. (1976). *J. Phys. Soc. Jpn*, **41**, 1707–1715.

HARDY, J. R. (1962). *Philos. Mag.* **7**, 315–335.

HOSHINO, S., FUJII, Y., HARADA, J. & AXE, J. D. (1976). *J. Phys. Soc. Jpn*, **41**, 965–973.

JASWAL, S. S. (1978*a*). *J. Phys. C*, **11**, 3559–3563.

JASWAL, S. S. (1978*b*). *Solid State Commun.* **27**, 969–971.

JASWAL, S. S. (1978*c*). *Proc. Int. Conf. on Lattice Dynamics*, edited by M. BALKANSKI, pp. 41–42. Paris: Flammarion.

KEPA, H. (1980). PhD Thesis, Warsaw.

KEPA, H., GIEBUŁTOWICZ, T., BURRAS, B., LEBECH, B. & CLAUSEN, K. (1982). To be published in *Phys. Scr.*

KUNC, K., BALKANSKI, M. & NUSIMOVICI, M. A. (1975*a*). *Phys. Status Solidi B*, **72**, 229–248.

KUNC, K., BALKANSKI, M. & NUSIMOVICI, M. A. (1975*b*). *Phys. Rev. B*, **12**, 4346–4355.

KUNC, K. & BILZ, H. (1976). *Solid State Commun.* **19**, 1027–1030.

KUNC, K. & NIELSEN, O. H. (1979*a*). *Comput. Phys. Commun.* **16**, 181–197.

KUNC, K. & NIELSEN, O. H. (1979*b*). *Comput. Phys. Commun.* **17**, 413–422.

KYUTT, R. N. (1975). *Sov. Phys. Crystallogr.* **19**(b), 705–708.

MATSUSHITA, T. & HAGASHI, J. (1977). *Phys. Status Solidi A*, **41**, 139–145.

MCINTYRE, G. J., MOSS, G. & BARNEA, Z. (1980). *Acta Cryst.* A**36**, 482–490.

MORLON, B., FUKAMACHI, T. & HOSOYA, S. (1981*a*). *Acta Cryst.* A**37**, 92–96.

MORLON, B., FUKAMACHI, T. & HOSOYA, S. (1981*b*). *Acta Cryst.* A**37**, C309.

MOSS, B., MCMULLAN, R. K. & KOETZLE, T. F. (1980). *J. Chem. Phys.* **73**(1), 495–508.

NIELSEN, O. H. & JASWAL, S. S. (1982). *Comput. Phys. Commun.* To be published.

NIELSEN, O. H., LARSON, F. K., DAMGAARD, S., PETERSEN, J. W. & WEYER, G. (1982). Submitted to *Phys. Status Solidi B.*

PLUMELLE, P., TALWAR, D. N., VANDEVYVER, M., KUNC, K. & ZIGONE, M. (1979). *Phys. Rev. B*, **20**, 4199–4212.

PLUMELLE, P. & VANDEVYVER, M. (1976). *Phys. Status Solidi B*, **73**, 271–281.

PREVOT, B. J. (1976). PhD Thesis, Strasbourg, Table IV-D.

PREVOT, B., HENNION, B. & DORNER, B. (1977). *J. Phys. C*, **10**, 3999–4011.

PRICE, D. L., ROWE, J. M. & NICKLOW, R. M. (1971). *Phys. Rev. B*, **3**, 1268–1279.

REID, J. S. (1981). *Acta Cryst.* A**37**, C258.

REID, J. S. & PIRIE, J. D. (1980). *Acta Cryst.* A**36**, 957–965.

ROWE, J. M., NICKLOW, R. M., PRICE, D. L. & ZANIO, K. (1974). *Phys. Rev. B*, **10**, 671–675.

SAKATA, M., HOSHINO, S. & HARADA, J. (1974). *Acta Cryst.* A**30**, 655–661.

TALWAR, D. N. & AGRAWAL, B. K. (1974). *J. Phys. C*, **7**, 2981–2988.

TALWAR, D. N., VANDEVYVER, M. & ZIGONE, M. (1980). *J. Phys. C*, **13**, 3775–3793.

VAGELATOS, N., WEHE, D. & KING, J. S. (1974). *J. Chem. Phys.* **60**, 3613–3618.

VALVODA, V. & JECNY, J. (1978). *Phys. Status Solidi A*, **45**, 269–275.

VANDEVYVER, M. & PLUMELLE, P. (1976). *J. Phys. Chem. Solids*, **38**, 765–777.

VANDEVYVER, M. & PLUMELLE, P. (1978). *Phys. Rev. B*, **17**, 675–685.

VETELINO, J. F., GAUR, S. P. & MITRA, S. S. (1972). *Phys. Rev. B*, **5**, 2360–2366.

WILLIS, B. T. M. & PRYOR, A. W. (1975). *Thermal Vibrations in Crystallography*. Cambridge Univ. Press.

YARNELL, J. L., WARREN, J. L., WENZEL, R. G. & DEAN, P. J. (1968). *Neutron Inelastic Scattering*, Vol. I, pp. 301–313. Vienna: IAEA.